Plasma cortisol is associated with cerebral hypometabolism across the Alzheimer's disease spectrum

Check for updates

Miranka Wirth [a,*,1], Catharina Lange [b,1], Willem Huijbers [c,1], for the Alzheimer's Disease Neuroimaging Initiative[2]

[a] German Center for Neurodegenerative Diseases (DZNE), Dresden, Germany
[b] Department of Nuclear Medicine, Charité - Universitätsmedizin Berlin, Corporate Member of Freie Universität Berlin, Humboldt-Universität zu Berlin, Berlin Institute of Health, Berlin, Germany
[c] Department of Cognitive Science and Artificial Intelligence, Tilburg University, Jheronimus Academy of Data Science, Tilburg, the Netherlands

ARTICLE INFO

ABSTRACT

Hypothalamic-pituitary-adrenal dysregulation is proposed as a risk factor for Alzheimer's disease (AD). This study assessed cross-sectional relationships between cortisol and neuroimaging biomarkers of brain structure and glucose metabolism across the AD spectrum. Participants with normal cognition, mild cognitive impairment, and AD were selected from the Alzheimer's Disease Neuroimaging Initiative databank, based on baseline measures of plasma cortisol, gray matter volume (n = 556), and cerebral glucose metabolism (n = 288). Relationships between plasma cortisol and the neuroimaging biomarkers were assessed. Across the entire cohort, higher plasma cortisol levels were associated with lower glucose metabolism in lateral and medial parietal regions. Higher plasma cortisol was also related to lower gray matter volume in temporal-parietal-occipital regions and in the hippocampus. There were no significant group differences in these relationships with adjustment for covariates. Our results demonstrate that hypothalamic-pituitary-adrenal axis activation is related to glucose hypometabolism within posterior cortical regions vulnerable to AD pathology. This regional pattern appears to be distinct from cortisol-related associations with brain structure. Future studies should delineate pathophysiological mechanisms underlying these effects.

© 2019 Elsevier Inc. All rights reserved.

1. Introduction

Stress, mediated by the hypothalamic-pituitary-adrenal (HPA) axis, has been proposed as a risk factor for the development of Alzheimer's disease (AD) (Machado et al., 2014). Known as the most important human glucocorticoid released by HPA axis activation, cortisol modulates homeostatic body functions, including negative feedback mechanisms in the brain (Martignoni et al., 1992). Elevated levels of circulating cortisol over time may, however, prompt brain injury and increase vulnerability to neurodegenerative diseases (de Kloet et al., 2005; Herbert et al., 2006; Sapolsky, 1996).

There is evidence to suggest that HPA axis activation and dysregulation may aggravate brain injury in regions sensitive to AD and, thereby, accelerate AD pathogenesis (Caruso et al., 2018; Machado et al., 2014). Cortisol levels, commonly measured in blood plasma/ serum, salvia, urine, or cerebrospinal fluid, are increased in patients with AD and mild cognitive impairment (MCI) (Martignoni et al., 1990; Popp et al., 2015). Higher cortisol concentrations are also related to lower gray matter (GM) volume, as assessed using magnetic resonance imaging (MRI). These negative associations are found in demented and dementia-free populations across the brain (Geerlings et al., 2015; Toledo et al., 2013) and in the hippocampus as a major region of interest (ROI; Huang et al., 2009; Lupien et al., 1998)—albeit with mixed results (Echouffo-Tcheugui et al., 2018; Kremen et al., 2010). Such brain alterations may contribute to higher risk of cognitive decline (Csernansky et al., 2006; Huang et al., 2009) and clinical progression (Ennis et al., 2017; Karlamangla et al., 2005; Popp et al., 2015) associated with stress hormone elevation.

By contrast, associations between circulating cortisol and cerebral glucose metabolism are largely unknown in the course of AD development. Decreased glucose metabolism within frontal-temporal-parietal association cortices, measured using 2-[F-18]-

* Corresponding author at: Deutsches Zentrum für Neurodegenerative, Erkrankungen e.V., Standort Dresden Tatzberg 41, 01307, Dresden, Germany. Tel.: +49351 210 463 601; fax: +49351 210 463 704.
E-mail address: miranka.wirth@dzne.de (M. Wirth).
[1] Equal contribution.
[2] Data used in preparation of this article were obtained from the Alzheimer's Disease Neuroimaging Initiative (ADNI) database (adni.loni.usc.edu). As such, the investigators within the ADNI contributed to the design and implementation of ADNI and/or provided data but did not participate in analysis or writing of this report. A listing of ADNI investigators has been submitted with this manuscript.

fluoro-2-deoxy-D-glucose (FDG) positron emission tomography (PET), is a key feature of prodromal and clinical AD (Friedland et al., 1983; Herholz, 2010; Minoshima et al., 1997). Chronic exposure to increased glucocorticoid concentration was formerly linked to impaired glucose metabolism in the hippocampus and other brain areas in rat models (Landgraf et al., 1978) as well as in hypercortisolemic patients with Cushing syndrome (Brunetti et al., 1998; Liu et al., 2016). Given these observations, we hypothesized that brain glucose metabolism may be affected by the actions of stress hormones along the AD spectrum.

The primary goal of the present cross-sectional study was to determine the unexplored relationship between plasma cortisol levels and cerebral glucose metabolism, measured using FDG PET, across the AD spectrum from cognitively normal older adults, to MCI, and clinical AD. In addition, we assessed the relationship between plasma cortisol and GM volume. Previous reports have focused on associations between plasma cortisol (and other cardiovascular risk factors) and global beta-amyloid (Aβ) burden (Toledo et al., 2012) as well as local GM volume (Toledo et al., 2013), using an overlapping sample from the Alzheimer's Disease Neuroimaging Initiative (ADNI) database. Our study aims to extend the important work by Toledo et al. (2013), as we examine the spatial distribution of cortisol-related associations across the two imaging modalities of brain structure (MRI) and brain metabolism (FDG PET).

2. Methods

Cross-sectional data used in this study were obtained from the ADNI database (adni.loni.usc.edu). The ADNI was launched in 2003 as a public-private partnership, led by Principal Investigator Michael W. Weiner, MD. The primary goal of ADNI has been to test whether serial MRI, PET, other biological markers, and clinical and neuropsychological assessment can be combined to measure the progression of MCI and early AD. For up-to-date information, see www.adni-info.org.

2.1. Participants

Participants were selected from the ADNI database (ADNI 1 cohort) with regard to availability of following assessments: (i) baseline plasma cortisol concentration, (ii) baseline structural (high-resolution T1-weighted) MRI, and baseline cerebral FDG PET (subgroup). Neuroimaging data were restricted to image data acquired within a time window of ±100 days anchored to the clinical baseline assessment (incl. collection of plasma cortisol data). The selection flowchart is depicted in Fig. 1.

The final sample included in this study had 556 participants with diagnostic labels of early dementia due to AD (n = 112), MCI in later stages (n = 386), and normal cognition (CN: n = 58). A subsample of 288 participants had FDG PET available (AD: n = 62, MCI: n = 200, and CN: n = 26).

Details on inclusion/exclusion criteria are available in the ADNI procedures manual (http://adni.loni.usc.edu/methods/documents/). Briefly, at the time of study enrollment, participants are of ages between 55 and 90 (inclusive) and have a Geriatric Depression Scale (GDS) score (Yesavage et al., 1982) less than 6, excluding individuals with depression. Other exclusion criteria comprise serious neurological disorders apart from possible AD, history of brain lesions or head trauma, and intake of psychoactive medication at baseline. Cognitively normal participants have a Mini−Mental State Examination (MMSE) (Folstein et al., 1975) score between 24 and 30 (inclusive), a Clinical Dementia Rating (CDR) Scale score (Morris, 1993) of 0, no memory complaints, and normal memory function. Participant with MCI have a MMSE score between 24 and 30 (inclusive), a

CDR score of 0.5, subjective memory complaints, objective memory dysfunction, and preserved general cognition and functional performance. Participants with AD demonstrate an initial MMSE score between 20 and 26 (inclusive), a CDR score of 0.5 or 1.0, and meet the National Institute of Neurological and Communicative Disorders and Stroke and the Alzheimer's Disease and Related Disorders Association criteria for clinically probable AD (McKhann et al., 2011).

Ethics approval was obtained by the ADNI investigators. All study participants provided written informed consent. The data that support the findings of this study are openly available in the ADNI database at adni.loni.usc.edu.

2.2. Acquisition and analysis of plasma cortisol

Plasma cortisol levels were provided by the Biomarkers Consortium Plasma Proteomics Project and extracted using the ADNImerge package. Blood samples were collected and interrogated in accordance with ADNI standard operating procedures detailed in the procedural manual (http://adni.loni.usc.edu/methods/). In brief, baseline plasma cortisol was quantified in overnight fasting (approximately 8 hours) blood samples, obtained from each participant in the morning before breakfast. The majority of
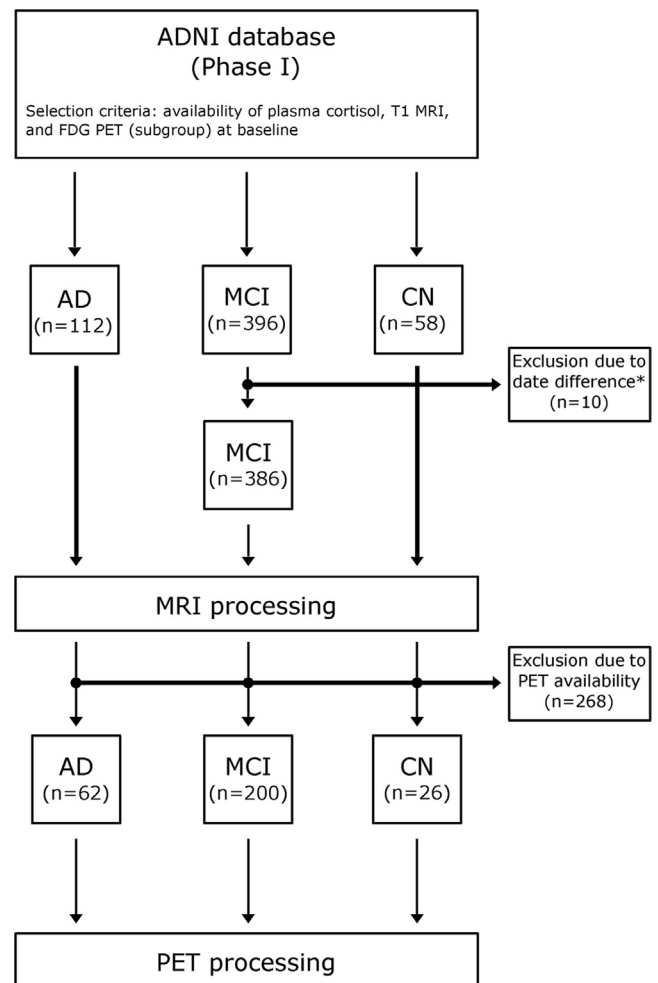

Fig. 1. Participant selection flowchart. The graph depicts the selection procedure from the ADNI database. *Selection of neuroimaging data was restricted to images acquired within a time window of ±100 days anchored to clinical baseline examinations. Abbreviations: AD, Alzheimer's disease; ADNI, Alzheimer's Disease Neuroimaging Initiative; FDG, 2-[F-18]-fluoro-2-deoxy-D-glucose; MCI, mild cognitive impairment; MRI, magnetic resonance imaging; CN, participants with normal cognition.

participants affirmed fasting for at least 6 hours (entire cohort: 92.1%, CN: 89.7%, MCI: 91.5%, and AD: 95.5%, with no significant group difference in these rates). For most blood samples, the time from collection to freezing was within 120 minutes. Whole-blood samples were collected into 10-mL BD lavender top K2EDTA-coated Vacutainer tubes and centrifuged within one hour after collection. Immediately after, blood plasma was transferred to a polypropylene transfer tube and placed in dry ice. Samples were shipped to the ADNI Biomarker Core Laboratory at the University of Pennsylvania. Following thawing at room temperature, 0.5 mL aliquots were prepared from plasma samples and stored in polypropylene aliquot tubes at −80°C until analyzed.

Plasma samples were interrogated by Rules-Based Medicine, Inc (Myriad RBM, Austin, TX) for levels of 190 analytes using a multiplex immunoassay panel. This panel, called the Human Discovery Multi-Analyte Profile (MAP), was developed on the Luminex xMAP platform by RBM. The analysis of plasma samples on the human discovery map is available on a commercial fee-for-service basis. Myriad RBM provides 3 levels of quality control (QC) for each analyte with details of QC results, detection limits for assays, and dynamic ranges for each plasma analytic shown in the data primer. Coefficients of variation (CVs) were calculated across plates for each analyte. Analytes were flagged, if replicates at one or more of the QC level repeats displayed CVs >25%, which was not the case for plasma cortisol. Assay information and quantification methods are described in the data primer (adni.loni.usc.edu/wp-content/uploads/2010/11/BC_Plasma_Proteomics_Data_Primer.pdf). Detailed documentation and validation reports are available from Myriad RBM (www.myriadrbm.com) and a previous report (Soares et al., 2012).

2.3. Acquisition and preprocessing of imaging data

2.3.1. Acquisition of MRI images

The MRI acquisition protocols were set up to harmonize image quality across MR hardware platforms (Jack et al., 2008a). In particular, high-resolution T1-weighted MR images were acquired on 1.5-Tesla MRI scanners using a sagittal 3-dimensional magnetization prepared rapid gradient echo sequence with an approximate repetition time = 2400 ms, minimum full echo time, inversion time = 1000 ms, and flip angle of 8° (scan parameters vary between sites, scanner platforms, and software versions).

2.3.2. Acquisition of FDG PET images

Cerebral FDG PET data were acquired on multiple PET scanners of varying resolutions. Platform-specific acquisition and reconstruction protocols were used to harmonize image quality across all ADNI centers (Jagust et al., 2010). FDG PET was performed according to a dynamic protocol resulting in 6 frames, each with a 5-minute duration from 30 to 60 minutes after injection.

2.3.3. Preprocessing of MRI images

The MRI images were downloaded from the ADNI repository as "unpreprocessed" data. Mcverter was used for DICOM-to-Nifti conversion (https://lcni.uoregon.edu/downloads/mriconvert/mriconvert-and-mcverter). For brain tissue segmentation into GM, white matter, and cerebrospinal fluid, the unified segmentation algorithm (Statistical Parametric Mapping, version SPM12; Wellcome Trust Centre for Neuroimaging, London, UK, www.fil.ion.ucl.ac.uk/spm) was deployed with default parameters, except that image data were resampled to 2 x 2 x 2 mm (Ashburner and Friston, 2005; Herron et al., 2012). Normalization to the Montreal Neurological Institute (MNI) template space was performed using diffeomorphic anatomical registration through exponentiated lie algebra (DARTEL) with default parameters and registration to "existing templates" (Ashburner, 2007). The IXI555 templates,

which are defined in MNI space and provided by the CAT12 toolbox, were used (http://dbm.neuro.uni-jena.de/vbm). Atlas-based hippocampal volumetry as well as voxel-wise statistical testing was performed on normalized and modulated GM images processed by DARTEL.

For ROI analysis, hippocampal volume was calculated. This was done using a previously published mask according to the EADC-ADNI Harmonized Protocol for hippocampal segmentation (HarP; probabilistic labels thresholded at 100% overlap) and inclusion of both modulated GM and white matter voxel values (Wolf et al., 2017). Total intracranial volume (TIV) was estimated by the method of Keihaninejad et al. (2010). Hippocampal volumes were corrected for TIV using a simple ratio. To conduct voxel-wise multiple regression analysis, the GM volume images were smoothed by a three-dimensional Gaussian kernel with full width at half maximum of 6 mm.

2.3.4. Preprocessing of FDG PET images

Reconstructed dynamic (or static, if dynamic was not available) PET data were downloaded from the ADNI repository in its original image format ("as archived," DICOM, Interfile, or ECAT). Image data were converted to Nifti, that is, from DICOM and ECAT using SPM12 or from Interfile using ImageConverter (version 1.1.5; Turku PET Centre). Preprocessing was performed fully automatically using a custom-made pipeline described elsewhere (Lange et al., 2015), except that the PET data were spatially normalized to MNI space using the parameter estimates from the MRI (see Section 2.3). The relative standardized uptake value (SUVr) was calculated voxel-wise using the whole-brain parenchyma as the reference region.

For ROI analysis, mean FDG SUVr was evaluated using an FDG-based AD template, which included parietal, temporal, and frontal regions. The template was defined previously from voxel-wise comparisons of FDG PET images in a largely independent ADNI sample of CN and patients with AD (except for 5 overlapping individuals) (Lange et al., 2015). For voxel-wise multiple regression analysis, SUVr images were smoothed by a three-dimensional Gaussian kernel with full width at half maximum of 12 mm.

2.4. Sample characteristics and covariates

2.4.1. Clinical data, neuropsychology, and APOE genotyping

Participants underwent comprehensive clinical and neuropsychological assessments. For the current analysis, we selected following clinical and neuropsychological measures from the ADNI database to describe the participant sample: individual baseline scores from the CDR Sum of Boxes, the MMSE, the Rey Auditory Verbal Learning Test, percent forgetting subscale (Rey, 1964), and the GDS.

In addition, the apolipoprotein E (APOE) genotype was selected from the ADNI database. The DNA extraction and genotyping were performed for study participants through analysis of blood samples that was carried out by the ADNI Biomarker Core Laboratory at the University of Pennsylvania.

2.4.2. Cardiovascular risk factor

To assess the influence of selected cardiovascular risk factors in our statistical models, we downloaded individual baseline scores of the following biomarkers from the ADNI database: systolic blood pressure, body mass index (BMI), and fasting glucose levels, as obtained before baseline FDG PET using a glucose meter on a drop of blood. In rare cases (n = 2), the BMI was not available at baseline assessment and was replaced by the BMI measured at screening.

2.5. Statistics

In general, statistical analyses of sample characteristics and ROI analysis were performed with IBM SPSS Statistics (version 24; IBM Corp., Armonk, NY, USA). Whole-brain data were visualized using Python (3.6.0) with the nibabel (DOI: 10.5281/zenodo.1464282) and nilearn (version 0.5.0b) modules. Scatter plots were generated using R (version 3.5.1) and ggplot2 (Wickham, 2016). Voxel-wise statistical testing was conducted in the Matlab environment (version R2013b; The MathWorks, Natick, USA).

2.5.1. Sample characteristics

The entire sample and each diagnostic group were characterized using baseline demographic, clinical, neuropsychological, and biomarker characteristics, including the APOE number of ε4 alleles (APOE4 status), the average FDG SUVr within the FDG AD template, total hippocampal volume, and plasma cortisol levels (raw values). Values were extracted from the ADNImerge data (R package), downloaded on April 17, 2018.

To evaluate possible group differences in sample characteristics, one-way analysis of variance (ANOVA) models were carried out with diagnostic group as an independent factor and the respective sample characteristic as a dependent variable. In case of a significant effect between groups, post hoc multiple comparisons were performed using either the Tukey's honestly significant difference test (assuming equal variance) or the Games Howell test (unequal variance).

2.5.2. Regions of interest analysis

The ROI analysis was performed in predefined ROIs, representing specific brain areas that are sensitively affected in patients with AD. For structural MRI, we assessed total volume of the bilateral hippocampi (TIV corrected), known to be sensitively reduced in patients with AD (Jack et al., 2008b). For FDG, we examined the mean SUVr in the combined FDG AD template, comprising neocortical areas, known to be hypometabolic in patients with AD (Lange et al., 2015).

In a first step, statistical analysis was conducted across the entire sample. Pearson correlation analysis was performed to evaluate relationships between plasma cortisol levels (transformed values using the logarithm function to conform data to normality) and each AD-sensitive ROI (MRI hippocampus, FDG AD template). In a follow-up analysis, we explored these relationships within each diagnostic group. Possible group differences were assessed, using one-way ANOVA models, which included each AD-sensitive ROI as a dependent variable and diagnostic groups (CN, MCI, and AD), plasma cortisol level, and their interactive term as independent factors. Scatter plots were created to visualize the relationships between plasma cortisol and glucose metabolism as well as GM volume measured in each preselected ROI, respectively. Correction for multiple comparisons was done using a false discovery rate (FDR)-adjusted p value of <0.05 (Benjamini and Hochberg, 1995).

2.5.3. Voxel-wise analysis

Voxel-wise regression analysis was run under SPM12 to evaluate relationships between plasma cortisol (log-transformed values) and imaging modalities (structural MRI and FDG) in the entire sample. Results were evaluated for significance at an FDR-adjusted p value of <0.05 and a minimum cluster size of 20 voxels. Analyses were adjusted for age and TIV (note: GM volume only) and restricted to cerebral GM using an explicit mask (cerebellum excluded). We did not adjust the voxel-wise analysis for additional covariates. To perform further analyses, average FDG SUVr and total GM volume were delineated from the combined

clusters of significant negative associations between plasma cortisol and the respective imaging modality (here referred as cortisol meta-ROI). For MRI, the cortisol meta-ROI values were corrected for TIV using a simple ratio.

Statistical analysis was first conducted across the entire sample, in a similar procedure described for the ROI analysis. Pearson correlation analysis was performed to examine the relationship between plasma cortisol levels (log-transformed values) and each cortisol meta-ROI (MRI, FDG). In a follow-up analysis, we explored these relationships within each diagnostic group. To assess possible group differences, one-way ANOVA models were computed with each cortisol meta-ROI as a dependent variable and diagnostic groups (CN, MCI, and AD), plasma cortisol, and their interactive term as independent variables. Scatter plots were created to visualize the relationships between plasma cortisol and glucose metabolism as well as GM volume measured in each cortisol meta-ROI, respectively. Correction for multiple comparisons was done, using an FDR-adjusted $p < 0.05$.

2.6. Adjustment for covariates

Our initial analyses were conducted without adjustment for covariates. In addition, we included statistical models with adjustment for age, gender, subclinical depression (measured using the GDS), APOE4 status, and cardiovascular risk factors of systolic blood pressure, BMI, and blood glucose levels (Note: Blood glucose levels were included only for statistical models with FDG PET). In case of missing data in any of the covariates (see Table 1), values were replaced by samples' mean for statistical analyses. In the result section, we report unadjusted and adjusted outcomes in the respective paragraphs.

3. Results

3.1. Characteristics of participants

Descriptive demographic, clinical, and biomarker characteristics are provided for the entire sample and within each diagnostic group in Table 1. Diagnostic groups were comparable in age, gender, and education. As expected, CN, MCI, and AD groups differed significantly in clinical measures, the APOE4 status, and the preselected AD-sensitive ROIs for FDG SUVr and GM volume. Plasma cortisol levels were significantly increased in patients with AD compared with the MCI group.

3.2. Results of ROI analyses

3.2.1. MRI ROI

Results of this ROI analysis are presented in Fig. 2 and Table 2A. Higher plasma cortisol was significantly related to lower hippocampal volume across entire cohort. When stratified by diagnostic group, a significant negative relationship between plasma cortisol and hippocampal volume was found only in the MCI group. There was, however, no significant interaction between diagnostic groups and plasma cortisol in the hippocampal ROI (F [2, 550] = 1.446, p = 0.236, n = 556). Adjustment for covariates did not change these results.

3.2.2. FDG ROI

Results of this ROI analysis are presented in Fig. 2 and Table 2A. Higher plasma cortisol levels were significantly related to lower glucose metabolism in the FDG AD template across the entire cohort. When stratified by diagnostic group, negative relationships between higher plasma and glucose metabolism were significant in the MCI and AD groups. There was a positive relationship between

Table 1
Baseline demographics, clinical, and biomarker characteristics

Characteristics	Entire cohort	CN	MCI	AD	*p*-value[d]
n (total)	556	58	386	112	
Demographics					
Age (y)	74.8 (7.4)	75.1 (5.8)	74.7 (7.4)	74.8 (8.0)	0.942
Gender (no. females)	213	28	138	47	0.126
Education (y)	15.6 (3.0)	15.7 (2.8)	15.7 (3.0)	15.1 (3.2)	0.185
Clinical measures					
CDR-SB	2.0 (1.6)	0.0 (0.1)	1.6 (0.9)	4.3 (1.6)	<0.001[a,b,c]
MMSE	26.6 (2.4)	28.9 (1.2)	27.1 (1.8)	23.6 (1.9)	<0.001[a,b,c]
RAVLT (% forgetting)	68.1 (33.3), n = 553	34.6 (33.9)	67.8 (31.4), n = 385	86.5 (24.2), n = 110	<0.001[a,b,c]
GDS	1.5 (1.4)	0.9 (1.2)	1.6 (1.4)	1.7 (1.34)	<0.001[b,c]
Biomarkers					
APOE4 status 0/1/2 (n: ε4 alleles)	271/216/69	53/5/0	182/158/46	36/53/23	<0.001[a,b,c]
Systolic blood pressure (mmHg)	133.4 (17.0), n = 554	131.4 (17.7)	133.2 (16.9), n = 384	135.0 (17.0)	0.401
BMI (kg/m²)	26.0 (3.9), n = 555	27.1 (4.1), n = 57	26.0 (4.0)	25.6 (3.8)	0.071
Blood glucose (mg/dL)	99.7 (16.4), n = 286	99.5 (15.7), n = 25	100.7 (17.6), n = 199	96.5 (11.9), n = 62	0.226
MRI hippocampus (mL)	5.2 (0.9)	5.8 (0.6)	5.2 (0.8)	4.7 (0.9)	<0.001[a,b,c]
FDG AD template	1.01 (0.04), n = 288	1.04 (0.02), n = 26	1.02 (0.03), n = 200	0.98 (0.05), n = 62	<0.001[a,b,c]
Plasma cortisol (ng/mL)	154.7 (53.5)	158.1 (60.8)	150.7 (53.3)	166.7 (48.4)	0.018[a]

Numbers are given if applicable as mean and standard deviation (parenthesis). The actual sample size is given, if different from sample size specified in first row.
Key: AD, participants with dementia due to Alzheimer's disease; ANOVA, analysis of variance; ApoE, apolipoprotein E; BMI, body mass index; CDR-SB, clinical dementia rating (sum of boxes); CN, participants with normal cognition; FDG, 2-[F-18]-fluoro-2-deoxy-D-glucose; n, number; GDS, Geriatric Depression Scale; MCI, participants with mild cognitive impairment; MMSE, Mini−Mental State Examination; MRI, magnetic resonance imaging; RAVLT, Rey Auditory Verbal Learning Test.
[a] Post hoc analysis: significant group difference between AD and MCI.
[b] Post hoc analysis: significant group difference between AD and CN.
[c] Post hoc analysis: significant group difference between MCI and CN.
[d] Statistical comparisons of numerical characteristics across diagnostic groups was performed by one-way ANOVA. In case of a significant effect between diagnostic groups, post hoc multiple comparisons were performed using either the Tukey's honestly significant difference test (assuming equal variance) or the Games Howell test (unequal variance). Chi-square statistic was used to compare the distribution of categorical variables between the 3 diagnostic groups. In case of a significant effect between groups, a chi-square test was applied to all possible pairs of groups. A significance level of $p < 0.05$ was assumed for between all group tests and for post hoc tests.

these 2 variables in the CN group ($p < 0.05$, uncorrected) and an interaction between diagnostic groups and plasma cortisol on glucose metabolism ($F [2, 282] = 3.749$, $p = 0.025$ uncorrected, n = 288). These relationships were not significant after correction for multiple comparisons and adjustment for covariates, suggesting that they might be due to chance.

3.3. Results of voxel-wise analyses

3.3.1. MRI

Results of this voxel-wise analysis are presented in Fig. 3 and Table 3. Higher plasma cortisol levels were related to lower GM volume across the entire sample. This negative relationship was
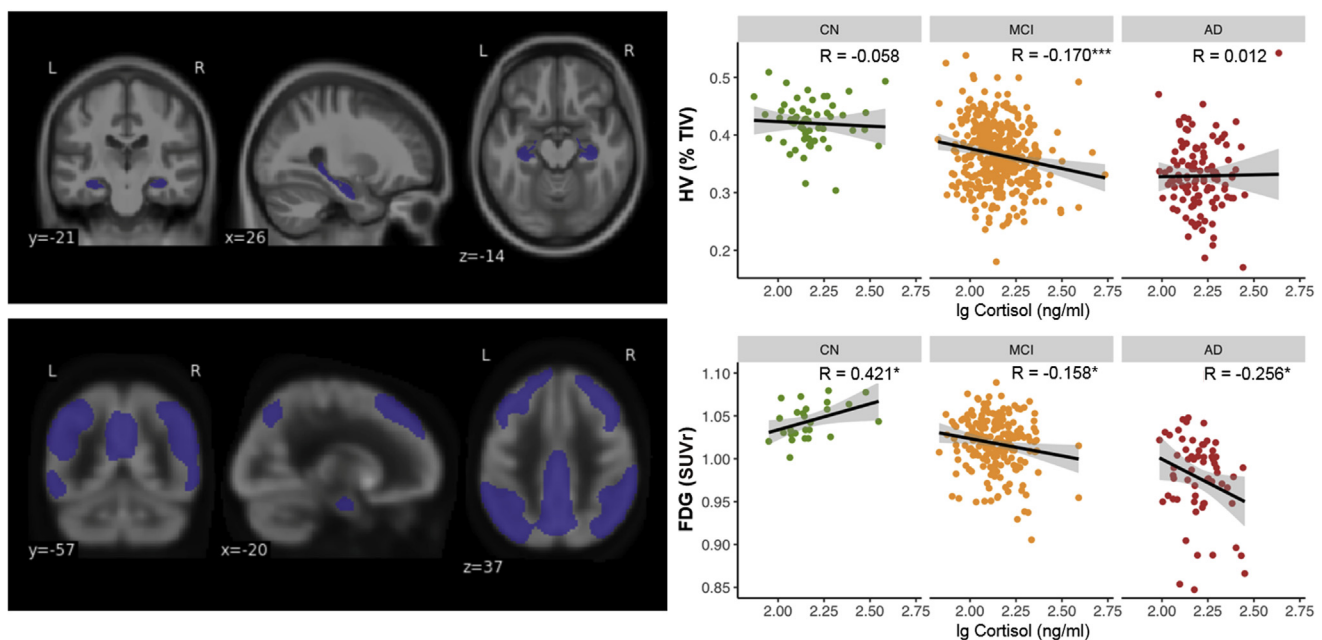

Fig. 2. Relationship between plasma cortisol, hippocampal volume, and glucose metabolism in preselected regions of interest. Top panel shows HV. Scatter plots (top right side) depict unadjusted relationships between plasma cortisol (log-transformed) and total HV (measured as % TIV). Lower panel shows glucose metabolism (FDG) from an a priori template, sensitive to AD pathology. Scatter plots (lower right side) depict relationships between plasma cortisol and average FDG SUVr. Dots represent individual data points, with CN in green and patients with MCI in orange and AD in red. Lines indicate linear trends within each diagnostic group, and gray area, the standard deviation. Correlation coefficients are provided in the top right for each diagnostic group. Significance levels (uncorrected): ***p < 0.001, * *p* < 0.05. Abbreviations: AD, Alzheimer's disease; CN, participants with normal cognition; FDG, 2-[F-18]-fluoro-2-deoxy-D-glucose; MCI, mild cognitive impairment; HV, hippocampal volume; SUVr, relative standardized uptake value; TIV, total intracranial volume. (For interpretation of the references to color in this figure legend, the reader is referred to the Web version of this article.)

Table 2
Relationship between plasma cortisol, gray matter volume, and glucose metabolism

	Entire cohort			CN			MCI			AD			p-value[c]
	n	*rho*	*p*-value	*n*	*rho*	*p*-value	*n*	*rho*	*p*-value	*n*	*rho*	*p*-value	
A. Preselected ROI													
MRI hippocampus (% TIV)	556	−0.143	0.001[a,b]	58	−0.058	0.666	386	−0.170	0.001[a,b]	112	0.012	0.899	0.236
	556[d]	−0.098	0.022[a,b]	58[d]	−0.004	0.967	386[d]	−0.112	0.029[a,b]	112[d]	−0.031	0.755	0.653
FDG AD template	288	−0.199	0.001[a,b]	26	0.421	0.032[a]	200	−0.158	0.025[a]	62	−0.256	0.045[a]	0.025[a]
	288[d]	−0.197	0.001[a,b]	26[d]	0.349	0.144	200[d]	−0.150	0.037[a]	62[d]	−0.286	0.034[a]	0.709
B. Cortisol meta-ROI													
MRI cortisol meta-ROI (% TIV)	556	-0.301	0.001[a,b]	58	−0.434	0.001[a,b]	386	-0.289	0.001[a,b]	112	−0.214	0.024[a,b]	0.747
	556[d]	−0.280	0.001[a,b]	58[d]	−0.426	0.002[a,b]	386[d]	-0.255	0.001[a,b]	112[d]	−0.216	0.026[a,b]	0.626
FDG cortisol meta-ROI	288	−0.274	0.001[a,b]	26	−0.180	0.379	200	−0.256	0.001[a,b]	62	−0.223	0.082	0.596
	288[d]	−0.278	0.001[a,b]	26[d]	−0.261	0.281	200[d]	-0.257	0.001[a,b]	62[d]	−0.212	0.120	0.677

Key: AD, participants with dementia due to Alzheimer's disease; ANOVA, analysis of variance; APOE, apolipoprotein E; CN, participants with normal cognition; FDG, 2-[F-18]-fluoro-2-deoxy-D-glucose; MCI, participants with mild cognitive impairment; MRI, magnetic resonance imaging; PET, positron emission tomography; ROI, regions of interest; TIV, total intracranial volume.

[a] $p < 0.05$ uncorrected.
[b] $p < 0.05$ false discovery rate (FDR)-adjusted for statistical tests performed within each imaging modality.
[c] Statistical comparisons across groups was performed by one-way ANOVA with each ROI as dependent variable and diagnostic group (CN, MCI, and AD), plasma cortisol, and their interactive term as independent factors.
[d] Statistical models adjusted for covariates of age, gender, subclinical depression, APOE status, and cardiovascular risk factors (Note: Blood glucose levels were included only for statistical models with FDG PET).

mainly found in temporal, temporo-parietal, and occipital regions of the left hemisphere. There was no significant positive relationship between plasma cortisol levels and GM volume at the given statistical threshold.

Follow-up analysis in the MRI cortisol meta-ROI was conducted. Results of this analysis are presented in Fig. 3 and Table 2B. Stratification by diagnostic group indicated that the negative relationship between plasma cortisol and GM volume in the MRI cortisol meta-
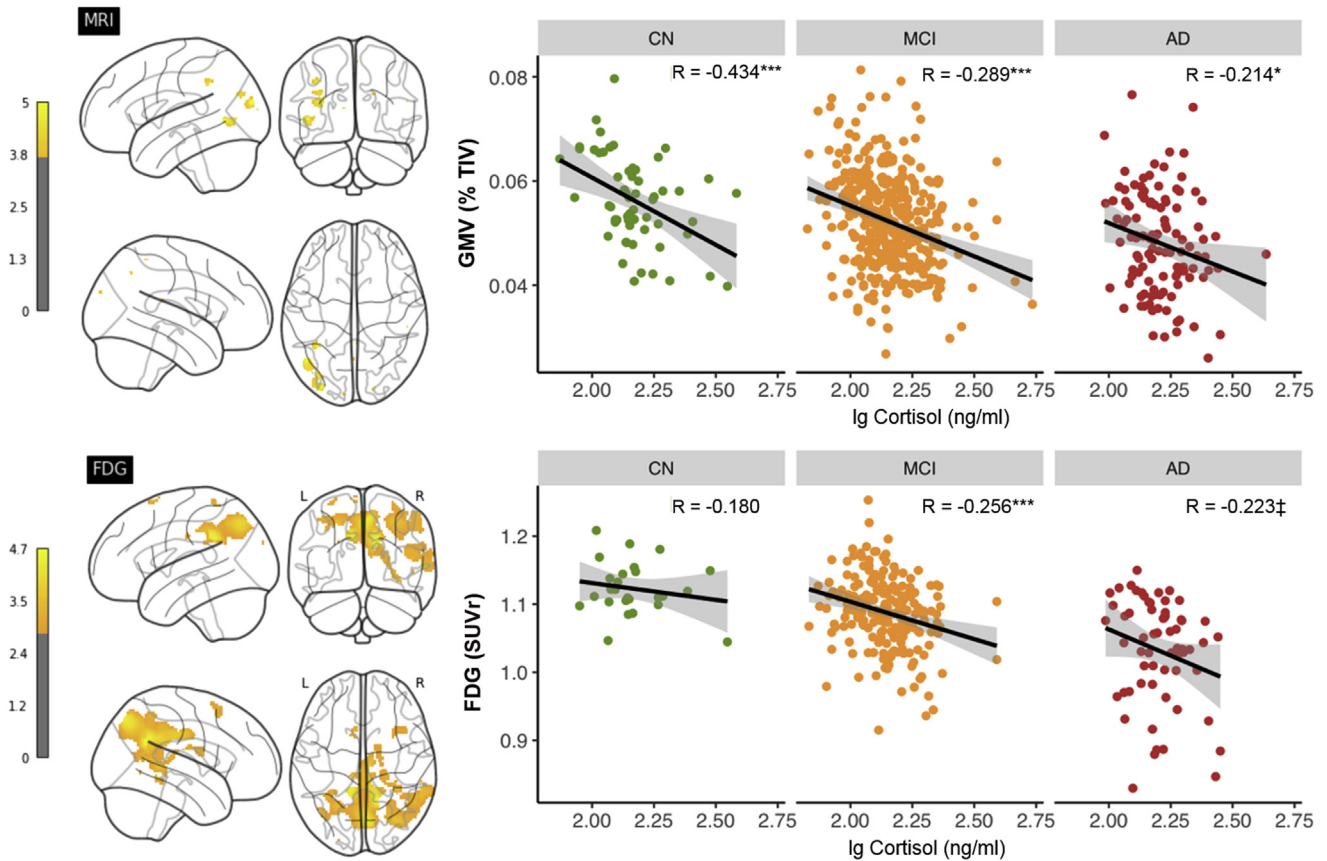

Fig. 3. Voxel-wise relationships between plasma cortisol, gray matter volume, and glucose metabolism. Top panel shows whole-brain analysis between cortisol and gray matter volume (MRI) and bottom panel between plasma cortisol (log-transformed) and glucose metabolism (FDG). Statistical maps (left side) are depicted on a glass brain. Color scales represent t-values starting at $p < 0.05$, corrected using false discovery rate. Scatter plots (right side) depict unadjusted relationships between plasma cortisol and total GMV (measured as % TIV) and average FDG SUVr within the corresponding cortisol meta-ROI. Dots represent individual data points, with CN in green and patients with MCI in orange and AD in red. Lines indicate linear trends within each diagnostic group, and gray area, the standard deviation. Correlation coefficients are provided in the top right for each diagnostic group. Significance levels (uncorrected): ***$p < 0.001$, * $p < 0.05$, ‡ $p < 0.1$. Abbreviations: AD, Alzheimer's disease; CN, participants with normal cognition; FDG, 2-[F-18]-fluoro-2-deoxy-D-glucose; MCI, mild cognitive impairment; MRI, magnetic resonance imaging; GMV, gray matter volume; SUVr, relative standardized uptake value; TIV, total intracranial volume. (For interpretation of the references to color in this figure legend, the reader is referred to the Web version of this article.)

Table 3
Significant clusters resulting from voxel-wise analysis of plasma cortisol against gray matter volume (corrected for age, TIV; n = 556)

Contrast	No. cluster	Cluster volume (mL)	Peak t-value	MNI x y z (mm)	Anatomical site
Negative	1	0.64	5.03	−47, −63, 2	Posterior temporal lobe, left
			4.00	−39, −71, 3	Lateral occipital lobe, left
	2	0.54	5.01	−33, −90, 20	Lateral occipital lobe, left
	3	0.19	4.85	−36, −48, 38	Inferior lateral parietal lobe, left
	4	0.22	4.46	−37, −80, 28	Lateral occipital lobe, left
Positive	-	-	-	-	*No suprathreshold clusters*

Anatomical specifications are provided for significant clusters ($p < 0.05$, FDR-adjusted) and a minimum cluster size of 20 voxels. Peak characteristics of each cluster are specified by their anatomical site (adapted version of Hammersmith atlas provided by CAT12 toolbox, Hammers et al., 2003), MNI coordinates, and t-value.
Key: FDR, false discovery rate; MNI x y z [mm], coordinates MNI space in millimeters; TIV, total intracranial volume.

ROI was significant within each diagnostic group. There was, however, no significant interaction between diagnostic groups and plasma cortisol (F [2, 550] = 0.292, p = 0.747, n = 556). Adjustment for covariates did not change these results.

3.3.2. FDG

Results of this voxel-wise analysis are presented in Fig. 3 and Table 4. Higher plasma cortisol levels were significantly related to lower cerebral glucose metabolism mainly across the entire cohort. This negative relationship was found in lateral temporo-parietal regions, the posterior cingulate, and medial parietal regions, including the precuneus of both hemispheres. There were no significant positive relationships between plasma cortisol levels and glucose metabolism at the given statistical threshold.

Follow-up analysis in the FDG cortisol meta-ROI was conducted. Results of this analysis are presented in Fig. 3 and Table 2B. Stratification by diagnostic group indicated that the negative relationship between plasma cortisol and glucose metabolism in the FDG cortisol meta-ROI was significant only in the MCI group. There was no significant interaction between diagnostic groups and plasma cortisol (F [2, 282] = 0.519, p = 0.596, n = 288). Adjustment for covariates did not change these results.

4. Discussion

This study demonstrated negative relationships between plasma cortisol and metabolic as well as structural brain biomarkers across the AD spectrum. Higher levels of circulating cortisol were associated with lower glucose metabolism in lateral and medial parietal brain regions. This regional pattern was somewhat distinct from cortisol-related relationships with GM structure. Although some of

the cortisol-related relationships appeared to be most pronounced in patients with MCI, we did not detect significant group differences with correction for multiple comparisons and adjustment for covariates. Our findings highlight that HPA axis activation is related to metabolic dysfunction in brain regions affected by AD, which may enhance vulnerability to AD development.

4.1. Plasma cortisol and cerebral glucose metabolism

We found that higher plasma cortisol was associated with lower brain glucose metabolism across the AD spectrum. This negative association was mainly seen within lateral temporo-parietal, medial parietal, and posterior cingulate regions of both hemispheres. In a similar line, data from animal models indicate that glucocorticoids may inhibit glucose metabolism within the hippocampus, but also other brain regions (Kadekaro et al., 1988; Landgraf et al., 1978). Using FDG PET, previous studies on patients with Cushing's syndrome have further related increased cortisol levels to global and regional patterns of perturbed cerebral metabolism (Brunetti et al., 1998; Liu et al., 2016). Conversely, de Leon et al. (1997) demonstrated that glucose metabolism was reduced in the hippocampus in response to hydrocortisone administration in normal older individuals. In the present study, we did not find a significant association between plasma cortisol and glucose metabolism in the hippocampus. Nevertheless, our findings confirm the notion that regional cerebral metabolism may be altered as a function of plasma cortisol.

The negative relationship between plasma cortisol and glucose metabolism was mainly observed in posterior cortical regions. These areas are known to be hypometabolic in prodromal and symptomatic stages of AD (Friedland et al., 1983; Minoshima et al., 1997; Wirth

Table 4
Significant clusters resulting from voxel-wise analysis of plasma cortisol against FDG (corrected for age; n = 288)

Contrast	No. cluster	Cluster volume (mL)	Peak t-value	MNI x y z (mm)	Anatomical site
Negative	1	25.6	4.72	14, −54, 28	Superior parietal gyrus, right
			4.44	−12, −44, 34	Superior parietal gyrus, left
			3.98	8, −36, 30	Posterior cingulate gyrus, right
			3.58	−4, −36, 40	Posterior cingulate gyrus, left
			3.36	−33, −50, 42	Inferior lateral parietal lobe, left
	2	3.54	3.70	58, −42, 2	Posterior temporal lobe, right
			3.18	60, -52, 22	Inferior lateral parietal lobe, right
	3	7.43	3.69	34, −72, 48	Inferior lateral parietal lobe, right
			3.21	36, −74, 36	Lateral occipital lobe, right
	4	0.25	3.44	34, −40, −8	Posterior temporal lobe, right
	5	0.79	3.28	24, -30, 14	Insula, right
			3.22	30, −38, −4	Posterior temporal lobe, right
	6	0.70	3.16	17, −10, 23	Caudate nucleus, right
	7	0.74	3.14	32, 16, 60	Middle frontal gyrus, right
Positive	-	-	-	-	*No suprathreshold clusters*

Anatomical specifications are provided for significant clusters ($p < 0.05$, FDR-adjusted) and a minimum cluster size of 20 voxels. Peak characteristics of each cluster are specified by their anatomical site (adapted version of Hammersmith atlas provided by CAT12 toolbox, Hammers et al., 2003), MNI coordinates, and t-value.
Key: FDG, 2-[F-18]-fluoro-2-deoxy-D-glucose; FDG, 2-[F-18]-fluoro-2-deoxy-D-glucose; FDR, false discovery rate; SUVr, relative standard uptake value (reference region: brain parenchyma); MNI x y z [mm], coordinates MNI space in millimeters.

et al., 2018). Neurophysiological mechanisms underlying the observed associations remain unclear. One possibility is that pathological pathways mediate the negative impact of HPA axis activation on metabolic dysfunctions in posterior cortical regions. For example, elevated glucocorticoid levels were previously linked to increased Aβ accumulation and tau hyperphosphorylation in rodents (Green et al., 2006; Wang et al., 2011) as well as global Aβ burden in humans, as assessed using a smaller ADNI sample (Toledo et al., 2012). In addition, other factors related to elevated stress hormone levels, such as increased blood pressure or blood glucose levels (Notarianni, 2017), may play a role in facilitating neural dysfunction in cortical regions. We and other groups (Kremen et al., 2010; Pietrzak et al., 2017) have adjusted statistical models for cardiovascular risk factors, with no impact on the overall results. However, a more detailed analysis of possible influences imposed by these risk factors on cortisol-related associations in larger samples will be needed.

Interestingly, we did not find significant associations between plasma cortisol and glucose metabolism in frontal brain regions across the AD spectrum. We had no specific hypothesis with regard to these particular regions and, therefore, can only provide a post hoc explanation. Despite the fact that our AD-sensitive FDG template included frontal areas (Lange et al., 2015), posterior cortical regions are really known to show the largest effect of hypometabolism in AD pathogenesis (Nestor et al., 2003). Frontal regions are more affected in advanced stages of the disease. Because our study included a larger number of participants at the prodromal disease stage, one may argue that there is greater disease-related variance in the posterior cortical regions. Therefore, these regions may be more likely to demonstrate cortisol-related associations in the present cohort.

4.2. Plasma cortisol and GM volume

Higher plasma cortisol levels were also associated with lower GM volume in the hippocampus and posterior cortical areas across the AD spectrum, as reported previously in an ADNI data set (Toledo et al., 2013). At the given statistical thresholds, mainly left lateral temporal-parietal-occipital regions were found. Notably, this spatial distribution was somewhat distinct from cortisol-related associations with cerebral metabolism. Our findings replicate existing reports, suggesting that circulating cortisol is associated with reduced GM volume, comprising (but not limited to) the hippocampus (Geerlings et al., 2015; Huang et al., 2009; Lupien et al., 1998) and posterior cortical areas (Echouffo-Tcheugui et al., 2018; Geerlings et al., 2015). Moreover, the cortisol-related associations within cortical areas were significant within each diagnostic group, which was not true for the hippocampus. Other studies have demonstrated similar negative associations between cortisol levels and cortical GM structure, even in dementia-free middle-aged adults (Echouffo-Tcheugui et al., 2018; Kremen et al., 2010). Thus, it appears that circulating glucocorticoids may affect neural structure through several neurodamaging pathways (Liston and Gan, 2011; McEwen et al., 2016) that could work before and independent of AD pathology. Such mechanisms may enhance susceptibility of the brain to aging and age-related neurodegenerative diseases.

4.3. Synopsis and outlook

Taken together, our findings are convergent with the idea that HPA axis activation may be a vigorous mechanism that accelerates brain injury associated with AD development (Caruso et al., 2018; Machado et al., 2014). We found that small but significant negative relationships between stress hormone levels and brain biomarkers may occur within regions sensitive to either hypometabolism or atrophy across the AD spectrum. Moreover, the present study replicated the well-documented existence of increased cortisol levels in clinical AD (Popp et al., 2009), yet only when comparing patients with AD to MCI. Clinical or lifestyle-based interventions could help to reduce elevated stress hormones levels at early disease stages and may thus potentially have a positive impact on disease progression. This hypothesis needs to be evaluated in future studies.

4.4. Strengths and limitations

Our study has strengths and limitations. The present results are based on the large and well-characterized ADNI cohort with standardized operation procedures that are publicly available. As a result, we were able to investigate plasma cortisol levels across the AD spectrum. However, the use of ADNI data is also a limitation, as our findings are not independent from a previous study investigating cortisol-related associations with GM structure (Toledo et al., 2013). The cross-sectional nature of assessments further precludes conclusions on the temporal sequence between HPA axis activation and brain injury associated with AD pathogenesis. Longitudinal studies including AD biomarkers will be needed to further evaluate cortisol-brain relationships.

We further acknowledge that cortisol levels are highly variable between individuals and also within the same individual over time. In the present study, plasma cortisol was obtained from a single assessment, which might not only reflect longer-term effects of high cortisol exposure, as opposed to dynamic measures over an extended time period. It therefore remains an open question, if our findings are mediated by the longer-term effects of circulating cortisol or by other factors that influence daily peaks in cortisol. Furthermore, plasma cortisol mostly reflects bound as opposed to unbound or free cortisol that is thought to be biologically active. A measure of free cortisol might thus provide a better estimate of stress-related function (Coolens et al., 1987; Fede et al., 2014). Finally, our findings are weighted toward the prodromal disease stage, with MCI patients being the largest participant group. Forthcoming studies are encouraged to assess relationships of cortisol exposure and brain biomarkers across the complete AD continuum.

5. Conclusion

In the present study, higher plasma cortisol levels were related with lower glucose metabolism in brain regions vulnerable to AD pathology across the disease spectrum. Higher plasma cortisol was also associated with lower regional GM volume, with a somewhat distinct regional distribution. The findings suggest that HPA axis activation could aggravate brain injury in regions that are affected by AD and thereby accelerate AD progression.

and Bioengineering, United States, and through generous contributions from the following: AbbVie; Alzheimer's Association; Alzheimer's Drug Discovery Foundation; Araclon Biotech; BioClinica, Inc; Biogen; Bristol-Myers Squibb Company; CereSpir, Inc; Eisai Inc; Elan Pharmaceuticals, Inc; Eli Lilly and Company; EuroImmun; F. Hoffmann-La Roche Ltd and its affiliated company Genentech, Inc; Fujirebio; GE Healthcare; IXICO Ltd; Janssen Alzheimer Immunotherapy Research & Development, LLC.; Johnson & Johnson Pharmaceutical Research & Development LLC.; Lumosity; Lundbeck; Merck & Co, Inc; Meso Scale Diagnostics, LLC.; NeuroRx Research; Neurotrack Technologies; Novartis Pharmaceuticals Corporation; Pfizer Inc; Piramal Imaging; Servier; Takeda Pharmaceutical Company; and Transition Therapeutics. The Canadian Institutes of Health Research is providing funds to support ADNI clinical sites in Canada. Private sector contributions are facilitated by the Foundation for the National Institutes of Health (www.fnih.org). The grantee organization is the Northern California Institute for Research and Education, and the study is coordinated by the Alzheimer's Disease Cooperative Study at the University of California, San Diego. ADNI data are disseminated by the Laboratory for Neuro Imaging at the University of Southern California.

Authors' contributions: MW contributed to study concept and design, data analysis, interpretation of study results, and manuscript drafting. CL contributed to data analysis, interpretation of study results, manuscript drafting, and final manuscript review. WH contributed to study concept and design, data analysis, interpretation of study results, manuscript drafting, and final manuscript review.

References

Ashburner, J., 2007. A fast diffeomorphic image registration algorithm. Neuroimage 38, 95−113.

Ashburner, J., Friston, K.J., 2005. Unified segmentation. Neuroimage 26, 839−851.

Benjamini, Y., Hochberg, Y., 1995. Controlling the false discovery rate: a practical and powerful approach to multiple testing. J. R. Stat. Soc. Ser. B (Methodological) 57, 289−300.

Brunetti, A., Fulham, M.J., Aloj, L., De Souza, B., Nieman, L., Oldfield, E.H., Di Chiro, G., 1998. Decreased brain glucose utilization in patients with Cushing's disease. J. Nucl. Med. 39, 786−790.

Caruso, A., Nicoletti, F., Mango, D., Saidi, A., Orlando, R., Scaccianoce, S., 2018. Stress as risk factor for Alzheimer's disease. Pharmacol. Res. 132, 130−134.

Coolens, J.L., Van Baelen, H., Heyns, W., 1987. Clinical use of unbound plasma cortisol as calculated from total cortisol and corticosteroid-binding globulin. J. Steroid Biochem. 26, 197−202.

Csernansky, J.G., Dong, H., Fagan, A.M., Wang, L., Xiong, C., Holtzman, D.M., Morris, J.C., 2006. Plasma cortisol and progression of dementia in subjects with Alzheimer-type dementia. Am. J. Psychiatry 163, 2164−2169.

de Kloet, E.R., Joels, M., Holsboer, F., 2005. Stress and the brain: from adaptation to disease. Nat. Rev. Neurosci. 6, 463−475.

de Leon, M.J., McRae, T., Rusinek, H., Convit, A., De Santi, S., Tarshish, C., Golomb, J., Volkow, N., Daisley, K., Orentreich, N., McEwen, B., 1997. Cortisol reduces hippocampal glucose metabolism in normal elderly, but not in Alzheimer's disease. J. Clin. Endocrinol. Metab. 82, 3251−3259.

Echouffo-Tcheugui, J.B., Conner, S.C., Himali, J.J., Maillard, P., DeCarli, C.S., Beiser, A.S., Vasan, R.S., Seshadri, S., 2018. Circulating cortisol and cognitive and structural brain measures: the Framingham Heart Study. Neurology 91, e1961−e1970.

Ennis, G.E., An, Y., Resnick, S.M., Ferrucci, L., O'Brien, R.J., Moffat, S.D., 2017. Long-term cortisol measures predict Alzheimer disease risk. Neurology 88, 371−378.

Fede, G., Spadaro, L., Tomaselli, T., Privitera, G., Scicali, R., Vasianopoulou, P., Thalassinos, E., Martin, N., Thomas, M., Purrello, F., Burroughs, A.K., 2014. Comparison of total cortisol, free cortisol, and surrogate markers of free cortisol in diagnosis of adrenal insufficiency in patients with stable cirrhosis. Clin. Gastroenterol. Hepatol. 12, 504−512 e8; quiz e23-4.

Folstein, M., Folstein, S., McHugh, P., 1975. "Mini-mental state": a practical method for grading the cognitive state of patients for the clinicians. J. Psychiatr. Res. 12, 189−198.

Friedland, R.P., Budinger, T.F., Ganz, E., Yano, Y., Mathis, C.A., Koss, B., Ober, B.A., Huesman, R.H., Derenzo, S.E., 1983. Regional cerebral metabolic alterations in dementia of the Alzheimer type: positron emission tomography with [18F] fluorodeoxyglucose. J. Comput. Assist. Tomogr 7, 590−598.

Geerlings, M.I., Sigurdsson, S., Eiriksdottir, G., Garcia, M.E., Harris, T.B., Gudnason, V., Launer, L.J., 2015. Salivary cortisol, brain volumes, and cognition in community-dwelling elderly without dementia. Neurology 85, 976−983.

Green, K.N., Billings, L.M., Roozendaal, B., McGaugh, J.L., LaFerla, F.M., 2006. Glucocorticoids increase amyloid-beta and tau pathology in a mouse model of Alzheimer's disease. J. Neurosci. 26, 9047−9056.

Herbert, J., Goodyer, I.M., Grossman, A.B., Hastings, M.H., de Kloet, E.R., Lightman, S.L., Lupien, S.J., Roozendaal, B., Seckl, J.R., 2006. Do corticosteroids damage the brain? J. Neuroendocrinol. 18, 393−411.

Herholz, K., 2010. Cerebral glucose metabolism in preclinical and prodromal Alzheimer's disease. Expert Rev. Neurotherapeutics 10, 1667−1673.

Herron, T., Kang, X., Woods, D., 2012. Automated measurement of the human corpus callosum using MRI. Front Neuroinform. 6, 25.

Huang, C.W., Lui, C.C., Chang, W.N., Lu, C.H., Wang, Y.L., Chang, C.C., 2009. Elevated basal cortisol level predicts lower hippocampal volume and cognitive decline in Alzheimer's disease. J. Clin. Neurosci. 16, 1283−1286.

Jack Jr., C.R., Bernstein, M.A., Fox, N.C., Thompson, P., Alexander, G., Harvey, D., Borowski, B., Britson, P.J., J, L.W., Ward, C., Dale, A.M., Felmlee, J.P., Gunter, J.L., Hill, D.L., Killiany, R., Schuff, N., Fox-Bosetti, S., Lin, C., Studholme, C., DeCarli, C.S., Krueger, G., Ward, H.A., Metzger, G.J., Scott, K.T., Mallozzi, R., Blezek, D., Levy, J., Debbins, J.P., Fleisher, A.S., Albert, M., Green, R., Bartzokis, G., Glover, G., Mugler, J., Weiner, M.W., 2008a. The Alzheimer's disease neuroimaging Initiative (ADNI): MRI methods. J. Magn. Reson. Imaging 27, 685−691.

Jack Jr., C.R., Lowe, V.J., Senjem, M.L., Weigand, S.D., Kemp, B.J., Shiung, M.M., Knopman, D.S., Boeve, B.F., Klunk, W.E., Mathis, C.A., Petersen, R.C., 2008b. 11C PiB and structural MRI provide complementary information in imaging of Alzheimer's disease and amnestic mild cognitive impairment. Brain 131 (Pt 3), 665−680.

Jagust, W.J., Bandy, D., Chen, K., Foster, N.L., Landau, S.M., Mathis, C.A., Price, J.C., Reiman, E.M., Skovronsky, D., Koeppe, R.A., Alzheimer's Disease neuroimaging Initiative, 2010. the Alzheimer's disease neuroimaging initiative positron emission tomography core. Alzheimers Dement 6, 221−229.

Kadekaro, M., Ito, M., Gross, P.M., 1988. Local cerebral glucose utilization is increased in acutely adrenalectomized rats. Neuroendocrinology 47, 329−334.

Karlamangla, A.S., Singer, B.H., Chodosh, J., McEwen, B.S., Seeman, T.E., 2005. Urinary cortisol excretion as a predictor of incident cognitive impairment. Neurobiol. Aging 26 (Suppl 1), 80−84.

Keihaninejad, S., Heckemann, R.A., Fagiolo, G., Symms, M.R., Hajnal, J.V., Hammers, A., Initi, A.s.D.N., 2010. A robust method to estimate the intracranial volume across MRI field strengths (1.5T and 3T). Neuroimage 50, 1427−1437.

Kremen, W.S., O'Brien, R.C., Panizzon, M.S., Prom-Wormley, E., Eaves, L.J., Eisen, S.A., Eyler, L.T., Hauger, R.L., Fennema-Notestine, C., Fischl, B., Grant, M.D., Hellhammer, D.H., Jak, A.J., Jacobson, K.C., Jernigan, T.L., Lupien, S.J., Lyons, M.J., Mendoza, S.P., Neale, M.C., Seidman, L.J., Thermenos, H.W., Tsuang, M.T., Dale, A.M., Franz, C.E., 2010. Salivary cortisol and prefrontal cortical thickness in middle-aged men: a twin study. Neuroimage 53, 1093−1102.

Landgraf, R., Mitro, A., Hess, J., 1978. Regional net uptake of 14C-glucose by rat brain under the influence of corticosterone. Endocrinol. Exp. 12, 119−129.

Lange, C., Suppa, P., Frings, L., Brenner, W., Spies, L., Buchert, R., 2015. Optimization of statistical single subject analysis of brain FDG PET for the prognosis of mild cognitive impairment-to-Alzheimer's disease conversion. J. Alzheimers Dis. 49, 945−959.

Liston, C., Gan, W.-B., 2011. Glucocorticoids are critical regulators of dendritic spine development and plasticity in vivo. Proc. Natl. Acad. Sci. 108, 16074−16079.

Liu, S., Wang, Y., Xu, K., Ping, F., Wang, R., Li, F., Cheng, X., 2016. Brain glucose metabolism is associated with hormone level in Cushing's disease: a voxel-based study using FDG-PET. Neuroimage Clin. 12, 415−419.

Lupien, S.J., de Leon, M., de Santi, S., Convit, A., Tarshish, C., Nair, N.P., Thakur, M., McEwen, B.S., Hauger, R.L., Meaney, M.J., 1998. Cortisol levels during human aging predict hippocampal atrophy and memory deficits. Nat. Neurosci. 1, 69−73.

Machado, A., Herrera, A.J., de Pablos, R.M., Espinosa-Oliva, A.M., Sarmiento, M., Ayala, A., Venero, J.L., Santiago, M., Villaran, R.F., Delgado-Cortes, M.J., Arguelles, S., Cano, J., 2014. Chronic stress as a risk factor for Alzheimer's disease. Rev. Neurosciences 25, 785−804.

Martignoni, E., Petraglia, F., Costa, A., Bono, G., Genazzani, A.R., Nappi, G., 1990. Dementia of the Alzheimer type and hypothalamus-pituitary-adrenocortical axis: changes in cerebrospinal fluid corticotropin releasing factor and plasma cortisol levels. Acta Neurol. Scand. 81, 452−456.

Martignoni, E., Costa, A., Sinforiani, E., Liuzzi, A., Chiodini, P., Mauri, M., Bono, G., Nappi, G., 1992. The brain as a target for adrenocortical steroids: cognitive implications. Psychoneuroendocrinology 17, 343−354.

McEwen, B.S., Nasca, C., Gray, J.D., 2016. Stress effects on Neuronal structure: Hippocampus, Amygdala, and prefrontal cortex. Neuropsychopharmacol. 41, 3−23.

McKhann, G.M., Knopman, D.S., Chertkow, H., Hyman, B.T., Jack Jr, C.R., Kawas, C.H., Klunk, W.E., Koroshetz, W.J., Manly, J.J., Mayeux, R., Mohs, R.C., Morris, J.C., Rossor, M.N., Scheltens, P., Carrillo, M.C., Thies, B., Weintraub, S., Phelps, C.H., 2011. The diagnosis of dementia due to Alzheimer's disease: recommendations from the National Institute on Aging-Alzheimer's Association workgroups on diagnostic guidelines for Alzheimer's disease. Alzheimers Dement 7, 263−269.

Minoshima, S., Giordani, B., Berent, S., Frey, K.A., Foster, N.L., Kuhl, D.E., 1997. Metabolic reduction in the posterior cingulate cortex in very early Alzheimer's disease. Ann. Neurol. 42, 85−94.

Morris, J.C., 1993. The Clinical Dementia Rating (CDR): current version and scoring rules. Neurology 43, 2412−2414.

Nestor, P.J., Fryer, T.D., Smielewski, P., Hodges, J.R., 2003. Limbic hypometabolism in Alzheimer's disease and mild cognitive impairment. Ann. Neurol. 54, 343−351.

Notarianni, E., 2017. Cortisol: Mediator of association between Alzheimer's disease and diabetes mellitus? Psychoneuroendocrinology 81, 129−137.

Pietrzak, R.H., Laws, S.M., Lim, Y.Y., Bender, S.J., Porter, T., Doecke, J., Ames, D., Fowler, C., Masters, C.L., Milicic, L., Rainey-Smith, S., Villemagne, V.L., Rowe, C.C.,

Martins, R.N., Maruff, P., 2017. Plasma cortisol, brain amyloid-β, and cognitive decline in preclinical Alzheimer's disease: a 6-year prospective cohort study. Biol. Psychiatry Cogn. Neurosci. Neuroimaging 2, 45–52.

Popp, J., Schaper, K., Kolsch, H., Cvetanovska, G., Rommel, F., Klingmuller, D., Dodel, R., Wullner, U., Jessen, F., 2009. CSF cortisol in Alzheimer's disease and mild cognitive impairment. Neurobiol. Aging 30, 498–500.

Popp, J., Wolfsgruber, S., Heuser, I., Peters, O., Hull, M., Schroder, J., Moller, H.J., Lewczuk, P., Schneider, A., Jahn, H., Luckhaus, C., Perneczky, R., Frolich, L., Wagner, M., Maier, W., Wiltfang, J., Kornhuber, J., Jessen, F., 2015. Cerebrospinal fluid cortisol and clinical disease progression in MCI and dementia of Alzheimer's type. Neurobiol. Aging 36, 601–607.

Rey, A., 1964. L'examen clinique en psychologie. Presses universitaires de France, Paris.

Sapolsky, R.M., 1996. Why stress is bad for your brain. Science 273, 749.

Soares, H.D., Potter, W.Z., Pickering, E., Kuhn, M., Immermann, F.W., Shera, D.M., Ferm, M., Dean, R.A., Simon, A.J., Swenson, F., Siuciak, J.A., Kaplow, J., Thambisetty, M., Zagouras, P., Koroshetz, W.J., Wan, H.I., Trojanowski, J.Q., Shaw, L.M., 2012. Plasma biomarkers associated with the apolipoprotein E genotype and Alzheimer disease. Arch. Neurol. 69, 1310–1317.

Toledo, J.B., Toledo, E., Weiner, M.W., Jack Jr., C.R., Jagust, W., Lee, V.M., Shaw, L.M., Trojanowski, J.Q., 2012. Cardiovascular risk factors, cortisol, and amyloid-beta deposition in Alzheimer's Disease Neuroimaging Initiative. Alzheimers Dement 8, 483–489.

Toledo, J.B., Da, X., Bhatt, P., Wolk, D.A., Arnold, S.E., Shaw, L.M., Trojanowski, J.Q., Davatzikos, C., 2013. Relationship between plasma analytes and SPARE-AD defined brain atrophy patterns in ADNI. PLoS One 8, e55531.

Wang, Y., Li, M., Tang, J., Song, M., Xu, X., Xiong, J., Li, J., Bai, Y., 2011. Glucocorticoids facilitate astrocytic amyloid-beta peptide deposition by increasing the expression of APP and BACE1 and decreasing the expression of amyloid-beta-degrading proteases. Endocrinology 152, 2704–2715.

Wickham, H., 2016. ggplot2: Elegant Graphics for Data Analysis. Springer-Verlag, New York.

Wirth, M., Bejanin, A., La Joie, R., Arenaza-Urquijo, E.M., Gonneaud, J., Landeau, B., Perrotin, A., Mezenge, F., de La Sayette, V., Desgranges, B., Chetelat, G., 2018. Regional patterns of gray matter volume, hypometabolism, and beta-amyloid in groups at risk of Alzheimer's disease. Neurobiol. Aging 63, 140–151.

Wolf, D., Bocchetta, M., Preboske, G.M., Boccardi, M., Grothe, M.J., Neuroimaging, A.s.D., 2017. Reference standard space hippocampus labels according to the European Alzheimer's Disease Consortium-Alzheimer's Disease Neuroimaging Initiative harmonized protocol: utility in automated volumetry. Alzheimers Demen. 13, 893–902.

Yesavage, J.A., Brink, T.L., Rose, T.L., Lum, O., Huang, V., Adey, M., Leirer, V.O., 1982. Development and validation of a geriatric depression screening scale: a preliminary report. J. Psychiatr. Res. 17, 37–49.